

The Dependence of Velocity and Clustering Statistics on Galaxy Properties

A. J. Benson^{1,3}, C. M. Baugh^{1,4}, S. Cole^{1,5}, C. S. Frenk^{1,6} and C. G. Lacey^{1,2,7}

1. Physics Department, University of Durham, Durham DH1 3LE, England.

2. SISSA, Astrophysics Sector, via Beirut, 2-4, 34014 Trieste, Italy.

3. E-mail: A.J.Benson@durham.ac.uk

4. E-mail: C.M.Baugh@durham.ac.uk

5. E-mail: Shaun.Cole@durham.ac.uk

6. E-mail: C.S.Frenk@durham.ac.uk

7. E-mail: lacey@sissa.it

arXiv:astro-ph/9910488v2 25 Aug 2000

31 January 2018

ABSTRACT

We use a combination of N-body simulations of the hierarchical clustering of dark matter and semi-analytic modelling of the physics of galaxy formation to probe the relationship between the galaxy distribution and the mass distribution in a flat, cold dark matter universe with mean density $\Omega_0 = 0.3$ (Λ CDM). We find that the statistical properties of the galaxy distribution in the model, as quantified by pairwise velocity dispersions and clustering strength, can be quite different from those displayed by the dark matter. The pairwise line-of-sight velocity dispersion of galaxies is sensitive to the number of galaxies present in halos of different mass. In our model, which is consistent with the observed galaxy number distribution, the galaxy velocity dispersion is $\sim 40\%$ lower than that of the dark matter and is in reasonable agreement with the values measured in the Las Campanas redshift survey by Jing et al. over two decades in pair separation. The origin of this offset is statistical rather than dynamical, and depends upon the relative efficiency of galaxy formation in dark matter halos of different mass. Although the model galaxies and the dark matter have markedly different correlation functions in real space, such biases conspire to cause the redshift space correlation functions to be remarkably similar to each other. Thus, although genuinely biased relative to the dark matter on small scales, the distribution of galaxies as seen in redshift space, appears unbiased. The predicted redshift-space galaxy correlation function agrees well with observations. We find no evidence in the model for a dependence of clustering strength on intrinsic galaxy luminosity, unless extremely bright galaxies, two magnitudes brighter than L_* , are considered. However, there are significant differences when model galaxies are selected either by morphology or by colour. Early type or red galaxies show a much stronger clustering amplitude than late type or blue galaxies, particularly on small scales, again in good agreement with observations.

Key words: large-scale structure of the Universe; galaxies:formation; galaxies:statistics.

1 INTRODUCTION

Measurements of the clustering and peculiar motions of galaxies can, in principle, reveal the way in which galaxies are related to the large-scale distribution of mass in the universe and thus provide strong tests of models of galaxy formation. In this paper we investigate three aspects of the galaxy distribution that are particularly sensitive to the galaxy-mass connection: the distribution of relative veloc-

ities of galaxy pairs, redshift-space distortions in statistical measures of galaxy clustering, and the dependence of clustering strength on intrinsic galaxy properties.

Most current discussion of large-scale structure takes place within the context of the cold dark matter (CDM) theory. It has long been known, however, that cold dark matter models in which the galaxies are assumed to have the same statistical distribution as the dark matter do not account for the relatively low *rms* pairwise velocity dispersion measured

in galaxy surveys. Indeed, the first N-body simulations of the standard CDM model (Davis et al. 1985) gave values 2–3 times higher than those that had been measured for galaxies in the CfA redshift survey by Davis & Peebles (1983). This conflict stimulated the development of the “high peak” model of galaxy formation (Bardeen et al. 1986), in which galaxies are assumed to be more strongly clustered than, and therefore to be biased tracers of, the dark matter distribution. In this case, mass fluctuations at the present day and the associated peculiar velocities are weaker than in an unbiased model with the same level of galaxy clustering. Davis *et al.* showed that galaxies identified with high peaks in the standard $\Omega_0 = 1$ CDM cosmology could approximately match the observed amplitude of galaxy clustering while having a velocity dispersion distribution only slightly higher than that measured by Davis & Peebles (1983) (and similar, in fact, to that in an $\Omega_0 = 0.2$ CDM model).

The observational determination of the pairwise velocity dispersion has been problematic. It is now recognized that this statistic is very sensitive to the contribution from galaxies in rich clusters, which were not fairly represented in early redshift surveys (Mo, Jing & Börner 1993, Zurek et al. 1994, Mo, Jing & Börner 1997, Somerville, Primack & Nolthenius 1997, Somerville, Davis & Primack 1997). More recent estimates from larger surveys, typically sampling volumes on the order of $10^6 h^{-3} \text{Mpc}^3$ [★], are more robust and in much better agreement with one another (Marzke et al. 1995, Jing, Mo & Börner 1998, Ratcliffe et al. 1998a). The current values are around $\sim 500 \text{ km s}^{-1}$, almost twice as large as the original measurement by Davis & Peebles (1983).

A complementary way to explore the connection between the distributions of dark matter and galaxies is to look for a dependence of clustering on galaxy properties such as intrinsic luminosity, morphology or colour. There have been many attempts to measure galaxy clustering as a function of luminosity, often with conflicting conclusions (Phillipps & Shanks 1987, Alimi, Valls-Gabaud & Blanchard 1988, Davis et al. 1988, Hamilton 1988, White, Tully & Davis 1988, Santiago & da Costa 1990, Iovino et al. 1993, Park et al. 1994). A number of recent measurements of the redshift-space correlation function of galaxies selected by absolute magnitude suggests a dependence of clustering strength on luminosity for galaxies brighter than L_* (Benoist et al. 1996, Tadros & Efstathiou 1996, Willmer, da Costa & Pellegrini 1998, Guzzo et al. 1999, but see Loveday et al. 1995 and Hoyle et al. 1999 for counter-examples).

A dependence of clustering on morphological type is, however, well established, with elliptical galaxies found to be more strongly clustered than spiral galaxies as measured both in angular catalogues (Davis & Geller 1976, Giovanelli, Haynes & Chincarini 1986, Iovino et al. 1993) and in three-dimensional surveys (Moore et al. 1994, Loveday et al. 1995). This result can be understood as a reflection of the morphology-density relation, the statement that elliptical galaxies preferentially inhabit high density regions of the Universe (Dressler 1980). The dependence of clustering on the colour of galaxies has also been measured in redshift surveys with the general consensus that red galaxies

are more strongly clustered than blue galaxies (Carlberg et al. 1997, Le Fèvre et al. 1996, Willmer, da Costa & Pellegrini 1998). This is, of course, related to the fact that elliptical galaxies are generally redder than spiral galaxies, and so this effect is due largely to the same physical processes that drive the morphological dependence of clustering. This colour dependence is not as clear cut for studies of the angular correlation function (Infante & Pritchett 1993, Landy, Szalay & Koo 1996), where the red and blue populations may have different redshift distributions.

In order to interpret the significance of these observational results, it is necessary to replace heuristic biasing schemes with physically motivated models that can realistically incorporate the role of the environment in the formation and evolution of galaxies. Semi-analytic models of galaxy formation (White & Frenk 1991, Kauffmann, White & Guiderdoni 1993, Lacey et al. 1993, Cole et al. 1994, Somerville & Primack 1998) follow the formation and evolution of galaxies *ab initio*, within the context of cosmological theories of structure formation. These models have met with significant successes in describing and predicting observed properties of galaxies, such as faint galaxy number counts (White & Frenk 1991, Kauffmann, Guiderdoni & White 1994, Baugh, Cole & Frenk 1996a), properties as a function of morphological type (Kauffmann 1996, Kauffmann, Charlot & White 1996, Baugh, Cole & Frenk 1996b) and the nature of Lyman break galaxies at high redshift (Baugh et al. 1998, Governato et al. 1998, Kolatt et al. 1999).

In their simplest implementation, semi-analytic models can give limited information about the clustering of galaxies on large scales (Baugh et al. 1999) by applying the analytic description of the clustering of dark matter halos developed by Mo & White (1996). A more powerful technique recently developed consists of incorporating the semi-analytic prescription into an N-body simulation, whereby the clustering of galaxies can be determined directly and reliably down to small scales (Kauffmann, Nusser & Steinmetz 1997, Kauffmann et al. 1999a, Kauffmann et al. 1999b, Benson et al. 2000, Diaferio et al. 1999). We applied such a technique in an earlier paper (Benson et al. 2000), and found that the semi-analytic model of Cole et al. (1999) produced a galaxy correlation function in a Λ CDM cosmology (i.e. a CDM model with $\Omega_0 = 0.3$ and $\Lambda/3H_0^2 = 0.7$) that matches remarkably well the real-space correlation function measured from the APM galaxy survey (Baugh 1996). On small scales, the model galaxies are less clustered than the dark matter. A similar conclusion was reached by Pearce et al. (1999) for galaxies formed in cosmological gas dynamics simulations and by Colín et al. (1999) for galactic dark matter halos formed in high-resolution N-body simulations.

In this paper, we combine our semi-analytic model of galaxy formation with high-resolution N-body simulations to investigate the clustering properties of galaxies selected according to various criteria. We consider clustering in real and redshift-space and show that galaxy velocity dispersions are significantly lower than those of the dark matter, in reasonable agreement with the data. Our results for this particular statistic differ somewhat from those recently obtained by Kauffmann et al. (1999a) and we explore the reasons for these differences. Kauffmann et al. also investigated the dependence of clustering amplitude on galaxy properties, finding that both early type and red galaxies were more

[★] We write the Hubble constant as $H_0 = 100h \text{ km s}^{-1} \text{ Mpc}^{-1}$.

strongly clustered than the galaxy population as a whole, in agreement with the work of Kauffmann, Nusser & Steinmetz (1997) and with the trends seen in the observational data. However, they found no evidence in their models for the luminosity dependent clustering amplitude measured by Willmer, da Costa & Pellegrini (1998). Our results for these properties are quite consistent with those of Kauffmann et al. (1999a), but we compare our models to different datasets.

The rest of the paper is laid out as follows. In §2, we briefly describe the semi-analytic model of galaxy formation and the N-body simulation used in this study. In §3 we describe how we take into account the effects of redshift space distortions and calculate galaxy velocity dispersions. We examine the model correlation functions of galaxies selected by luminosity, morphology and colour and compare these results with the available observational data in §4. Finally, in §5 we present our conclusions.

2 DESCRIPTION OF THE NUMERICAL TECHNIQUE

We implement the semi-analytic model of Cole et al. (1999) in the ‘‘GIF’’ N-body simulations, a full description of which may be found in Jenkins et al. (1998) and Kauffmann et al. (1999a). These are high-resolution dark matter simulations that follow 17 million particles within a cosmological cubical volume of side $141.3h^{-1}$ Mpc. In this paper, we focus attention on the Λ CDM simulation, which has cosmological parameters, $\Omega_0 = 0.3$, $\Lambda/(3H_0^2) = 0.7$, $h = 0.7$, a power spectrum shape parameter $\Gamma = 0.21$, and normalisation $\sigma_8 = 0.9$ (to match the local abundance of hot X-ray clusters; White, Efstathiou & Frenk 1993, Eke, Cole & Frenk 1996.) Dark matter halos are identified using the friends-of-friends algorithm (Davis et al. 1985) with a linking length of 0.2 times the mean interparticle separation. We consider only halos consisting of ten or more particles, which Kauffmann et al. (1999a) have shown are stable clusters in the GIF simulations, and correspond to a lower halo mass limit of $1.4 \times 10^{11}h^{-1}M_\odot$. Benson et al. (2000) have shown that galaxy catalogues produced by the semi-analytic model with this halo mass limit are complete for galaxies brighter than $M_B - 5 \log h \approx -18.3$. The semi-analytic model populates the simulated volume with approximately 12,000 galaxies brighter than $M_B - 5 \log h = -19.5$.

In order to investigate the clustering properties of very bright, low abundance galaxies we have used a different simulation of a much larger volume. This was carried out by the VIRGO Consortium and hereafter we will refer to it as the ‘‘512³’’ simulation. It has identical cosmological parameters to the GIF Λ CDM simulation, although the initial conditions were generated using the transfer function calculated from CMBFAST (Seljak & Zaldarriaga 1996) rather than the fitting function of Bond & Efstathiou (1984) which was used for the GIF simulations. The simulated volume is a cube of side $479h^{-1}$ Mpc, populated with 134 million particles, giving a particle mass of $6.8 \times 10^{10}h^{-1}M_\odot$. Resolving halos of 10 or more particles in this simulation results in galaxy catalogues which are complete for galaxies brighter than $M_B - 5 \log h \approx -20.3$. Thus, we will only use this simulation for studying the distribution of the very brightest galaxies.

We have found that the clustering strength of the dark matter in the 512³ simulation is slightly larger than in the GIF simulation at large pair separations. The ratio of the real-space dark matter correlation functions in the two simulations, $\xi_{512^3}/\xi_{\text{GIF}}$, is 1.4 at pair separations of $10h^{-1}$ Mpc, decreasing to 1.1 at $4h^{-1}$ Mpc, and becoming unity at $2h^{-1}$ Mpc. This difference is due primarily to finite volume effects in the GIF simulation, which is missing some of the large-scale power included in the 512³ simulation. This deficit is carried through into the galaxy correlation functions. It should be noted, however, that this effect does not invalidate the conclusions of Benson et al. (2000) and, if anything, it slightly improves the agreement between our models and the APM correlation function on scales greater $\gtrsim 10h^{-1}$ Mpc.

We use the same implementation of the semi-analytic galaxy formation model described in detail by Benson et al. (2000) to populate our simulations with galaxies. Briefly, for each dark matter halo identified in the simulation at the redshift of interest, a Monte-Carlo merger history is generated, based upon the extended Press & Schechter formalism (Press & Schechter 1974, Bond et al. 1991, Bower 1991, Lacey & Cole 1993, Cole et al. 1999). A set of simple, physically motivated rules that describe the galaxy formation process is then applied to the merger history. The physics modelled include:

- (i) the radiative cooling of virialised gas in halos;
- (ii) the depletion of the resulting reservoir of cold gas by star formation;
- (iii) the feedback arising from stellar winds and supernovae that regulate the supply of cold gas;
- (iv) the chemical enrichment of the gas and stars;
- (v) the mergers of galaxies due to dynamical friction.

The star formation history of each galaxy is then used to determine its magnitude in any required band. The effect of dust extinction is determined using the models of Ferrara et al. (1999) as described by Cole et al. (1999) where full details of the semi-analytic modelling can be found.

Our fiducial model is essentially the same as that of Cole et al. (1999), whose parameters are set by the requirement that the model should reproduce, as closely as possible, a variety of properties of the local galaxy population, with particular emphasis placed on the shape and amplitude of the local, b_J -band luminosity function measured in the ESO Slice Project (ESP) by Zucca et al. (1997). Two cosmological parameters, σ_8 and Γ , differ slightly in this work from the values used by Cole et al. (1999). This is simply because Cole et al. had the freedom to choose these values (they selected $\sigma_8 = 0.93$ and $\Gamma = 0.19$) whereas we are restricted to using the values employed in the GIF Λ CDM simulation. These small differences have no significant effect on any of the results presented here. Since Cole et al. (1999) used the Press-Schechter mass function for dark matter halos, whereas we use the mass function produced by the GIF Λ CDM simulation, we altered slightly the star formation efficiency, ϵ_* , in the model in order to obtain as good a match to the luminosity function as Cole et al. did. Specifically, we set $\epsilon_* = 0.01$, whereas Cole et al. (1999) chose $\epsilon_* = 0.0067$.

The semi-analytic model identifies the most massive galaxy in each halo as the central galaxy, onto which radiatively cooling gas is focussed. This galaxy is placed at the

centre of mass of the simulated halo, and is given the peculiar velocity of the centre of mass. Satellite galaxies in the halo are assigned the position and peculiar velocity of randomly chosen dark matter particles within the halo. In this way, satellite galaxies always trace the dark matter within a given halo.

The technique that we employ differs in two important respects from that used by Kauffmann et al. (1999a). Firstly, Kauffmann et al. extract the full merger history of each dark matter halo directly from the N-body simulation. Although this approach has the advantage that the evolution of any individual galaxy can be followed through the simulation, the properties of the merger histories generated by the Monte-Carlo method are statistically equivalent to those obtained directly from the N-body simulation (but have superior mass resolution). In particular, the merger histories in the N-body simulation are found not to correlate with environment, in agreement with the assumptions of the Monte-Carlo approach (Somerville et al. 1998, Lemson & Kauffmann 1999). As a result, any statistical properties such as the correlation function, are not affected by the differences between the two approaches. Secondly, Kauffmann et al. adjusted the parameters of their semi-analytic model to match the zero-point of the Tully-Fisher relation between spiral galaxy luminosity and rotation speed rather than the observed luminosity function as we do. As a result, some of their models give a poor match to the luminosity function. Benson et al. (2000) have argued that a good match to the luminosity function is required for a robust estimate of the correlation function which, furthermore, for Λ CDM provides a good match to the data.

Our semi-analytic model also follows the evolution of galaxy morphology, as described in Baugh, Cole & Frenk (1996b) and Cole et al. (1999), a feature that we exploit in §4.2 to investigate the dependence of clustering strength on morphology. In the model, virialised gas cools to form a rotationally supported disk and quiescent star formation turns this gas into stars. A galactic bulge can be built up through the accretion of relatively small satellite galaxies or as the result of a violent merger between galaxies of comparable mass. In the latter case, any material in a disk is rearranged into a bulge and a burst of star formation occurs if cold gas is present. The morphology of a galaxy can thus change with time and is related to its environment, which determines both the rate at which gas cools and the merger rate between galaxies.

3 REDSHIFT SPACE DISTORTIONS

The clustering of galaxies in real space cannot be measured directly unless a distance indicator is available that does not rely on redshift. However, the real space clustering can be inferred indirectly, by deprojecting either the correlation function measured in terms of projected galaxy separation or the angular correlation function (e.g. Peebles 1980). In the case of noisy projected measurements, both methods require assumptions about the form of the two-point correlation function in real space, whilst the second method also requires knowledge of the redshift distribution of galaxies.

The three dimensional correlation function in redshift-space can be measured directly, by inferring the radial posi-

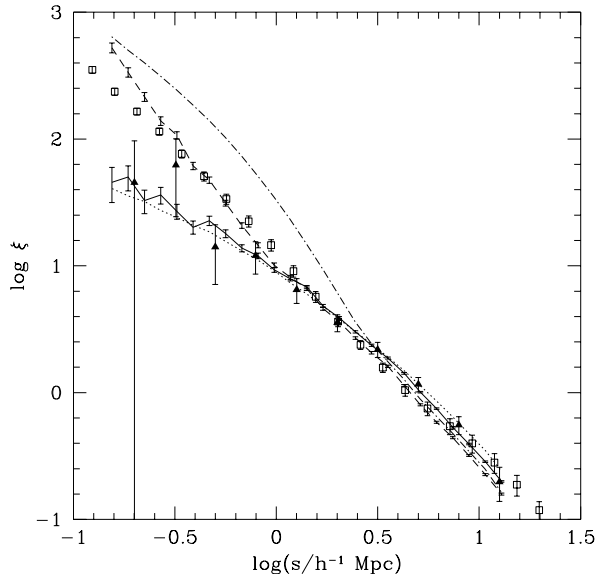


Figure 1. Real and redshift-space correlation functions in the Λ CDM model. The redshift-space correlation function of model galaxies brighter than $M_B - 5 \log h = -19.5$ is shown as a solid line, while the redshift-space correlation function of dark matter is shown as a dotted line. The dashed and dot-dashed lines show the real space correlation functions for galaxies and dark matter respectively. Error bars on the galaxy correlation functions are derived from Poisson statistics. The symbols with error bars are observational determinations of the galaxy correlation function: triangles show the redshift-space correlation function of galaxies brighter than $M_B - 5 \log h = -19.5$ from the ESO Slice Project (Guzzo et al. 1999), whilst squares show the real-space galaxy correlation function from the APM survey (Baugh 1996).

tion of each galaxy from its redshift, assuming a uniform Hubble flow. However, galaxies have peculiar motions in addition to the Hubble flow, induced by inhomogeneities in the local density field. This leads to a modification of the apparent pattern of galaxy clustering, commonly referred to as ‘redshift-space distortions’. Generally, these distortions reduce the strength of clustering on small scales, where the motion of galaxies within virialised structures tends to smear out galaxy positions inferred from redshifts (creating ‘Fingers of God’), and boost the strength of clustering on large scales where galaxies experience coherent flows into overdense regions and out of underdense regions (Kaiser 1987, Hamilton 1992). The redshift-space galaxy correlation function in our model therefore depends on both the spatial distribution of the galaxies and their distribution of peculiar velocities. We will comment on uncertainties that this introduces in §3.2.

The redshift-space clustering of galaxies in the simulation is straightforward to compute from the position and peculiar velocity of each galaxy. Redshift space positions are calculated by adding v_x/H_0 to the x coordinate of each galaxy, where v_x is the x -component of the peculiar velocity of that galaxy. This gives the redshift space position (at $z = 0$), as viewed by an observer located at infinity. From the resulting catalogue we can compute clustering statistics in the usual way.

In Fig. 1 we show the two-point correlation function

of galaxies brighter than $M_B - 5 \log h = -19.5$ in redshift space. The figure also shows the real-space correlation function for comparison. The two effects of redshift-space distortion described above are readily apparent in this figure. In real space the galaxy correlation function has an almost power-law form between 0.1 and $10h^{-1}$ Mpc, with a slope of $\gamma \approx -1.8$. In redshift-space, the galaxy correlation function falls below this power-law on small scales, whereas on scales larger than a few megaparsecs, it rises above it.

Kaiser (1987) showed that the amplification in redshift-space of the two-point correlation function on large scales due to coherent inflow onto large-scale structures is approximately a factor of $1 + \frac{2}{3}\beta + \frac{1}{5}\beta^2$, where $\beta = \Omega_0^{0.6}/b$ and b is the galaxy bias, assumed to be independent of scale. For the model considered here, $\Omega_0 = 0.3$, and the galaxies are essentially unbiased on large scales. The amplification factor is therefore ~ 1.37 . Whilst Kaiser's expression assumes $\Lambda_0 = 0$, in practice a non-zero cosmological constant makes very little difference, merely increasing the amplification factor to 1.39 (Lahav et al. 1991). The value measured for our galaxies at separations of $10h^{-1}$ Mpc, where linear theory is still a fair approximation, is 1.27 ± 0.04 , in reasonable agreement with the analytic expectation.

It is remarkable that whilst galaxies and dark matter have very different two-point correlation functions in real space, on scales smaller than $3h^{-1}$ Mpc the redshift-space correlation functions of galaxies and dark matter are almost indistinguishable. This implies that galaxies and dark matter have different velocity dispersions on these scales, and suggests that estimates of galaxy bias obtained from clustering in redshift space should be treated with caution.

3.1 Galaxy peculiar motions

Pairwise velocity statistics for dark matter and galaxies are plotted in Fig. 2. The data points in the figure were obtained from the Las Campanas Redshift Survey (hereafter LCRS, Shectman et al. 1996) by Jing, Mo & Börner (1998). Following Jenkins et al. (1998), a quantity that may be compared to these data is the projected, line-of-sight velocity dispersion given by:

$$\sigma_{\text{los}}^2(r_p) = \frac{\int \xi(r) \sigma_{\text{proj}}^2(r) dl}{\int \xi(r) dl}, \quad (1)$$

where r_p denotes projected separation, l distance along the line of sight, $r = \sqrt{r_p^2 + l^2}$, and the integral is taken along the line-of-sight between $\pm\infty$, although in practice convergence is attained with integration limits of $\pm 25h^{-1}$ Mpc. The quantity σ_{proj}^2 is the line-of-sight pairwise dispersion, which is given by:

$$\sigma_{\text{proj}}^2 = \frac{r_p^2 \langle v_{\perp}^2 \rangle / 2 + l^2 (\langle v_{\parallel}^2 \rangle - \langle v_{21} \rangle^2)}{r_p^2 + l^2}, \quad (2)$$

where $\langle v_{\perp}^2 \rangle^{1/2}$ is the rms relative pairwise velocity perpendicular to the vector connecting each pair, \mathbf{r}_{12} , $\langle v_{\parallel}^2 \rangle^{1/2}$ is the rms relative pairwise peculiar velocity along \mathbf{r}_{12} and $\langle v_{21} \rangle$ is the mean relative pairwise peculiar velocity along \mathbf{r}_{12} , all of which are functions of $r = |\mathbf{r}_{12}|$.

The line-of-sight velocity dispersion of the *dark matter*, shown in the left-hand panel of Fig. 2, is significantly

larger than the value for LCRS galaxies on small scales. At $r \sim 0.5h^{-1}$ Mpc, the observed value is $535 \pm 100 \text{ km s}^{-1}$, whereas for the dark matter $\sigma_{\text{los}} = 870 \text{ km s}^{-1}$. For dark matter, we find that the measured σ_{los} from the GIF simulation is in good agreement with that obtained by Jenkins et al. (1998) from a simulation of a volume approximately 5 times larger than the GIF simulation and from that in the 512^3 simulation, differing by less than 50 km s^{-1} on all scales considered here.

To compare to the LCRS data we have constructed a sample of galaxies brighter than $M_R - 5 \log h = -21.5$ which corresponds approximately to the apparent magnitude limit of the LCRS at its mean depth of $300h^{-1}$ Mpc. The line-of-sight velocity dispersion of these *galaxies*, shown in the right-hand panel by the thick solid line, is in reasonable agreement with the data. A sample selected to have $M_B - 5 \log h \leq -19.5$ has a very similar σ_{los} , as shown by the thin solid line in the right-hand panel.

Fig. 2 shows that model galaxies display a markedly different velocity dispersion from the dark matter on all the scales considered. This "velocity bias" is statistical in origin, and is unrelated to dynamical friction in clusters, because each galaxy in our model is assigned the peculiar velocity of a particle belonging to a dark matter halo in the N-body simulation. This effect arises because the galaxy distribution does not constitute a Poisson sampling of the dark matter distribution. Firstly, L_* galaxies are found only in dark matter halos more massive than $\sim 10^{12}h^{-1}M_{\odot}$, whereas a significant fraction of the dark matter is in smaller mass objects. Secondly, the number of galaxies in each halo is not in direct proportion to the halo mass, as would be required for Poisson sampling (Benson et al. 2000). The number of galaxies per halo determines how well the velocity structure of the halo is traced by the galaxy distribution. Our results for galaxy velocity dispersions differ somewhat from those found by Kauffmann et al. (1999a) using a similar technique. In §3.2 we explore thoroughly the causes of these differences.

The kind of biases seen in the pairwise velocity dispersion function are also present in single galaxy statistics. Fig. 3 shows the three-dimensional velocity dispersion of galaxies and dark matter within spheres of radius r , measured relative to the mean velocity within the sphere. At large r , this quantity tends to a constant value, the rms peculiar velocity of individual galaxies. As the figure shows, the dispersion within spheres is lower for galaxies than for dark matter and, furthermore, it depends on galaxy luminosity. For bright galaxies, the velocity dispersion is about 20% lower than for the dark matter. The dependence on luminosity arises because the fainter sample contains relatively more galaxies in the most massive halos which have the largest velocity dispersions. The figure also shows that the sampling variance of the velocity dispersion function is very large, particularly on small scales. For example, for sphere radii of $10h^{-1}$ Mpc, velocities as low as $\sim 100 \text{ km s}^{-1}$, are within $1-\sigma$ of the mean dispersion. This reflects the importance of long wavelength density fluctuations in determining the small-scale velocity field.

3.2 Comparison to previous work

The pairwise galaxy velocity dispersions that we find are somewhat lower than those obtained by Kauffmann et al.

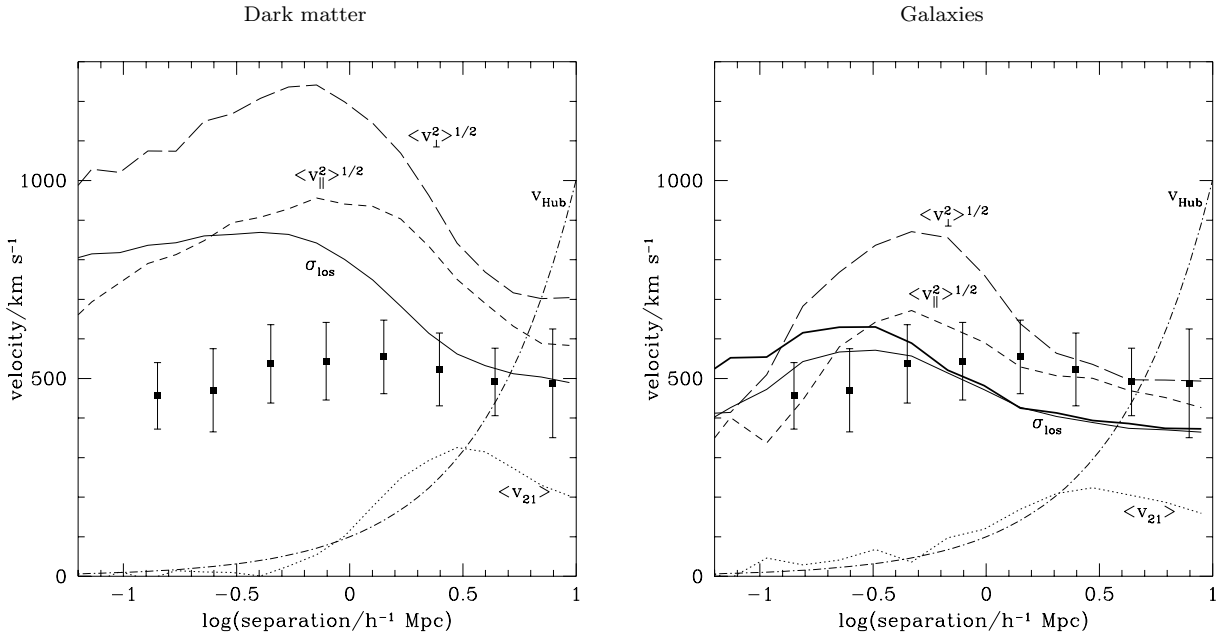


Figure 2. Pairwise velocities of dark matter particles (left-hand panel) and galaxies (right-hand panel) measured in the Λ CDM simulation. The dotted line is the mean inward radial peculiar velocity of pairs, $\langle v_{21} \rangle$; the short-dashed line is the rms pairwise radial peculiar velocity, $\langle v_{\parallel}^2 \rangle^{1/2}$; the long-dashed line is the rms pairwise perpendicular peculiar velocity, $\langle v_{\perp}^2 \rangle^{1/2}$; the solid lines are the rms pairwise line-of-sight peculiar velocity, σ_{los} ; and the dot-dash line is the Hubble expansion given by $v_{\text{Hub}} = -H_0 r$, where H_0 is Hubble's constant and r is physical separation. In the right hand panel the thick solid line shows σ_{los} for a sample with $M_B - 5 \log h \leq -21.5$, whilst all other lines are for a sample of galaxies with $M_B - 5 \log h \leq -19.5$. The data points with error bars are taken from Jing, Mo & Börner (1998) and show the pairwise velocity dispersion, σ_{12} , estimated for the Las Campanas redshift survey. The error bars are the square root of the sum in quadrature of the errors derived from the data and 1σ uncertainties inferred from mock catalogues by Jing et al. These points should be compared to the line-of-sight dispersions, σ_{los} , for the models (solid lines). Data points and σ_{los} are plotted against projected separation, r_p , whilst all other curves are plotted against true separation, r .

(1999a) using exactly the same N-body simulations as us, but a different semi-analytic prescription. Kauffmann et al found very similar (to within 10%) pairwise velocities for dark matter particles and galaxies on all scales. Thus, unlike ours, their model disagrees with the Jing, Mo & Börner (1998) data. Since the two semi-analytic treatments attempt to model the same physics, it is instructive to understand the reasons for this discrepancy.

The first, and most obvious difference is that Kauffmann et al. (1999a) considered galaxies one magnitude fainter than we do and the pairwise velocities are higher for fainter galaxies (because fainter samples consist of proportionally more satellite galaxies in clusters than brighter cuts). In our model, the line-of-sight velocity dispersion, σ_{los} , of galaxies brighter than $M_B - 5 \log h = -18.5$ is approximately 150 km s⁻¹ higher than that for galaxies one magnitude brighter. However, as may be seen in Fig. 4, even for galaxies of the same luminosity, there is still a discrepancy between our results and those of Kauffmann et al. There are three effects that could give rise to this discrepancy: (i) different assignments of peculiar velocities and/or positions to galaxies in the same halo; (ii) differences in the frequency with which the two semi-analytic models populate a halo of given mass with a particular number of galaxies; and (iii) statistical variations in the formation histories of galaxies in halos of a given mass. We have carried out several tests of these effects.

The results of the tests are shown in Fig. 4. The thick

solid line shows σ_{los} for the dark matter in the GIF simulation, whilst the thin solid line shows σ_{los} for galaxies brighter than $M_B - 5 \log h \leq -19.5$ in our model. In order to estimate the variance arising from different galaxy formation histories, we have generated ten realisations of our model using different random number sequences when constructing dark matter merger trees and selecting random halo particles on which to place the galaxies. The variation in σ_{los} between these ten models is an underestimate of the true statistical uncertainty because the population of dark matter halos is, of course, identical in all ten realizations. The dashed line shows σ_{los} for galaxies in our model brighter than $M_B - 5 \log h \leq -18.5$, with 1σ error bars derived in this way. Although σ_{los} for these galaxies is larger than for our brighter sample, it is still biased relative to the dark matter and is significantly below the Kauffmann et al. result. Thus, statistical uncertainties and magnitude selections, although relatively large, do not, on their own, explain the difference between the two semi-analytic models.

We now consider differences in the way in which the two models assign positions and velocities to galaxies within a given halo. In our model, each galaxy is assigned the position and velocity of a randomly chosen dark matter halo particle (except the central galaxy which is assigned the position and velocity of the centre of mass of the halo). In the model of Kauffmann et al. (1999a), galaxies initially form on the most bound particle in their halo. If that halo later merges with a larger one, the galaxy becomes a satellite in the new

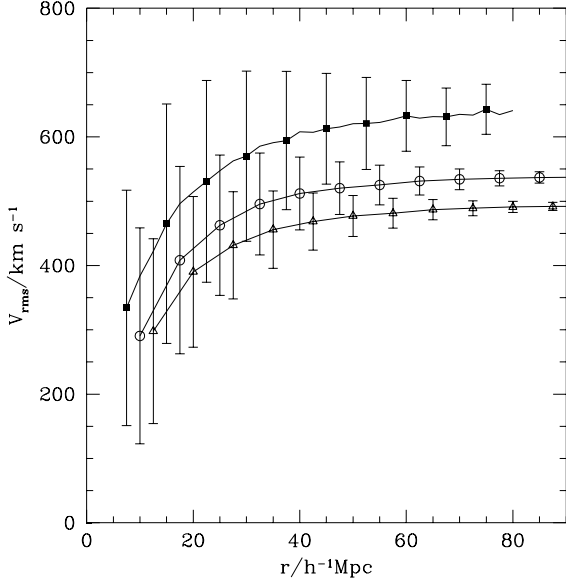


Figure 3. The three-dimensional velocity dispersion of individual galaxies and dark matter in spheres of radius r measured relative to the mean velocity within the sphere. Filled squares show the velocity dispersion of the dark matter, whilst open symbols show the velocity dispersion of galaxies brighter than $M_B - 5 \log h = -19.5$ (triangles) and $M_B - 5 \log h = -18.5$ (circles). The symbols indicate the mean velocity dispersion, and the error bars show the rms scatter in this quantity.

halo and remains attached to the dark matter particle on which it formed. Diaferio et al. (1999) have shown that this placement scheme leads to a dynamical velocity bias, such that blue galaxies in clusters have a higher velocity dispersion than the cluster dark matter because they preferentially occupy particles which are in the process of falling into the cluster for the first time. Such dynamical biases cannot (by construction) arise in our model.

To test the effect of the different placement schemes, we have taken the galaxy catalogue of Kauffmann et al. (limited at $M_B - 5 \log h = -18.5$ and kindly provided by A. Diaferio) and identified the dark matter halo of the GIF simulation to which each of these galaxies belongs. We have then assigned positions and velocities to these galaxies using our own placement scheme. The resulting σ_{los} is shown in Fig. 4 as the dot-dashed line (with error bars calculated from ten realisations of the placement scheme). This may be compared to the σ_{los} for the original Kauffmann et al. catalogue shown as the dotted line. The two curves are very similar on small scales and the small differences that there are on scales larger than $1h^{-1}$ Mpc are, in fact, due to our choice of always siting one galaxy at the centre of mass of each halo. (When we place *all* the Kauffmann et al. galaxies on randomly chosen halo particles the two curves agree extremely well on all scales.) This test demonstrates that the differences between our results and those of Kauffmann et al. are not due to the different ways in which galaxies are identified with dark matter halo particles in the two models.

We conclude that the differences between our results and those of Kauffmann et al. must be due to the frequency with which halos of different mass are populated with a par-

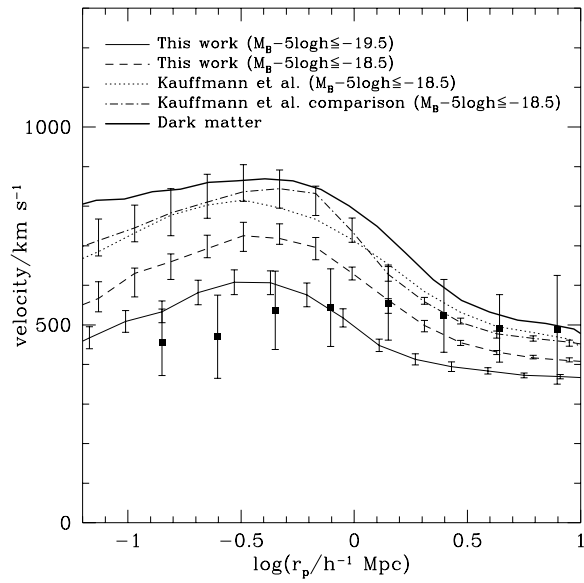


Figure 4. Line-of-sight velocity dispersions, σ_{los} for: dark matter (thick solid line); galaxies in our model that are brighter than $M_B - 5 \log h = -19.5$ (thin solid) and $M_B - 5 \log h = -18.5$ (dashed line); galaxies in the model of Kauffmann et al. (1999a) that are brighter than $M_B - 5 \log h = -18.5$ (dotted line); the Kauffmann et al. galaxies but with positions and velocities assigned using our placement scheme (dot-dashed line). The error bars on these lines reflect sampling uncertainties in the simulated volume as discussed in the text. Squares with error bars are estimated from the Las Campanas Redshift Survey (Jing, Mo & Börner 1998).

ticular number of galaxies in the two semi-analytic models. This statistic is shown in Fig. 5. Our model and that of Kauffmann et al. agree well for halos below $\sim 10^{13}h^{-1}M_\odot$, but for higher masses Kauffmann et al. assign systematically more galaxies to each halo (typically around 30% more) than we do. Thus, the catalogue of Kauffmann et al. gives greater weight to the most massive, highest velocity dispersion halos to which pairwise statistics are quite sensitive. As a result, they predict significantly higher velocity dispersions than we do. Since the $10^{15}h^{-1}M_\odot$ bin contains only three halos in the GIF simulation, we also show our model predictions (filled symbols) from an independent sample of twenty halos of mass $10^{15}h^{-1}M_\odot$ populated using exactly the same galaxy formation rules (indicated by filled symbols). For comparison, we have indicated in the figure the number of galaxies brighter than $M_B - 5 \log h = -19.5$ found in the Coma cluster and the corresponding number in our model. The virial mass and radius of the Coma cluster are $0.8 \pm 0.1 \times 10^{15}h^{-1}M_\odot$ and $1.5h^{-1}\text{Mpc}$ (1.2°) respectively (Geller, Diaferio & Kurtz 1999). Within a circular aperture of this radius centred on NGC4874, Godwin, Metcalfe & Peach (1983) find 100 galaxies brighter than $M_B - 5 \log h = -18.5$ and 25 galaxies brighter than $M_B - 5 \log h = -19.5$ (at the fainter magnitude cut a contamination of approximately 5.5 field galaxies is expected). Although this sample of one cluster cannot be used to confirm our model, it is consistent with our predicted distribution of galaxy numbers but also with that predicted by Kauffmann et al. To differentiate between these two models

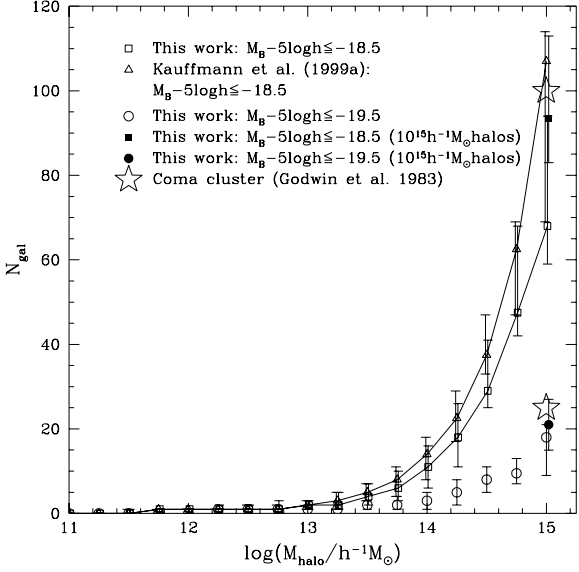


Figure 5. The number of galaxies per halo brighter than $M_B - 5 \log h = -18.5$ as a function of halo mass in our model (squares) and that of Kauffmann et al. (1999a) (triangles). Also shown is the number of galaxies per halo brighter than $M_B - 5 \log h = -19.5$ as a function of halo mass in our model (circles). Filled symbols show the corresponding predictions from our model for an independent sample of twenty $10^{15} h^{-1} M_\odot$ halos. The symbols show the median of the distribution whilst error bars indicate the 10% and 90% intervals of the distribution. The number of galaxies brighter than $M_B - 5 \log h = -18.5$ and -19.5 within the virial radius of the Coma cluster as found by Godwin, Metcalfe & Peach (1983) are indicated by stars.

would require a larger observational sample of rich clusters. Our model has been shown to be in good agreement with the observed total luminosities of groups and clusters determined by Moore, Frenk & White (1993) (Figure 16 of Benson et al. 2000), indicating that it is populating both groups and clusters with galaxies in a realistic fashion.

Although velocity statistics are sensitive to the numbers of galaxies placed in high mass halos, we have checked that galaxy correlation functions (in both real and redshift-space) are much less affected. For example, the redshift-space correlation function of galaxies brighter than $M_B - 5 \log h \leq -18.5$ differs by only 10% on scales of $10 h^{-1} \text{Mpc}$ and by less than 20% on scales of $0.3 h^{-1} \text{Mpc}$ when estimated using the number of galaxies per halo predicted by our model and by that of Kauffmann et al. (1999a). This is comparable to the scatter between models with different parameters found by Benson et al. (2000).

Fig. 6 shows the effects of varying key model parameters on the pairwise velocity dispersions. In §4.1 we describe these models further and explain our criteria for rejecting models as being non-realistic. Of the fifteen variants considered, five would be classed as non-realistic, and are shown as dashed lines. These models show a greater spread in velocity dispersions than the viable models (solid lines) which have only a small scatter around the fiducial model. This demonstrates that robust predictions for velocity dispersions can be made once non-realistic models are excluded.

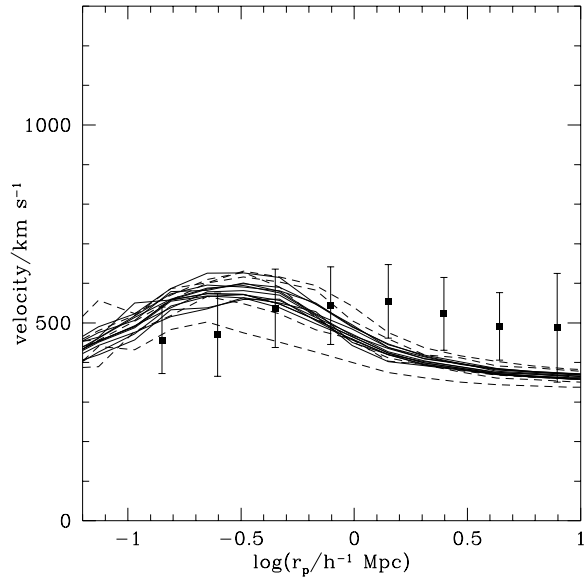


Figure 6. The line-of-sight pairwise velocity dispersion, σ_{los} , for galaxies with $M_B - 5 \log h \leq -19.5$. The lines show fifteen variants of our fiducial model in which some of the key parameters have been varied. The five models shown as dashed lines would be rejected as being non-realistic, as discussed in §4.1. The data points with error bars are taken from Jing, Mo & Börner (1998) and show the pairwise velocity dispersion, σ_{12} , estimated for the Las Campanas redshift survey.

4 THE DEPENDENCE OF CLUSTERING ON GALAXY PROPERTIES

We now examine the clustering properties of various subsamples extracted from our original galaxy catalogue, selecting by luminosity, morphology or colour.

4.1 Dependence of clustering on luminosity

In Fig. 7 we show our predicted redshift-space correlation functions for four cuts in absolute magnitude, and compare them with the corresponding correlation functions measured in the ESP redshift survey by Guzzo et al. (1999). (The space density of galaxies in our model at each of these magnitude cuts matches closely that found in the ESP survey, since our b_J -band luminosity function is tuned to agree with the ESP survey — c.f. Fig 11). The error bars on the model are estimates of the sample variance, computed in the following manner. For each magnitude cut, we extract fifty randomly placed cubes from our simulation which have a volume equal to that of the corresponding volume-limited samples drawn from the ESP survey. For the ESP survey volume-limited at $M_{b_J} - 5 \log h \leq -18.5, -19.5$ and -20.5 , our simulation volume contains 46, 17 and 6 independent survey volumes respectively. Thus, for the brighter samples our estimates of the sample variance is likely to be an underestimate of the true value. In the figure, we plot the median correlation function of these fifty realisations, and error bars showing the 10% and 90% intervals of the distribution. As can be seen, the model results are in excellent agreement with the data over the whole range of scales and magnitudes shown.

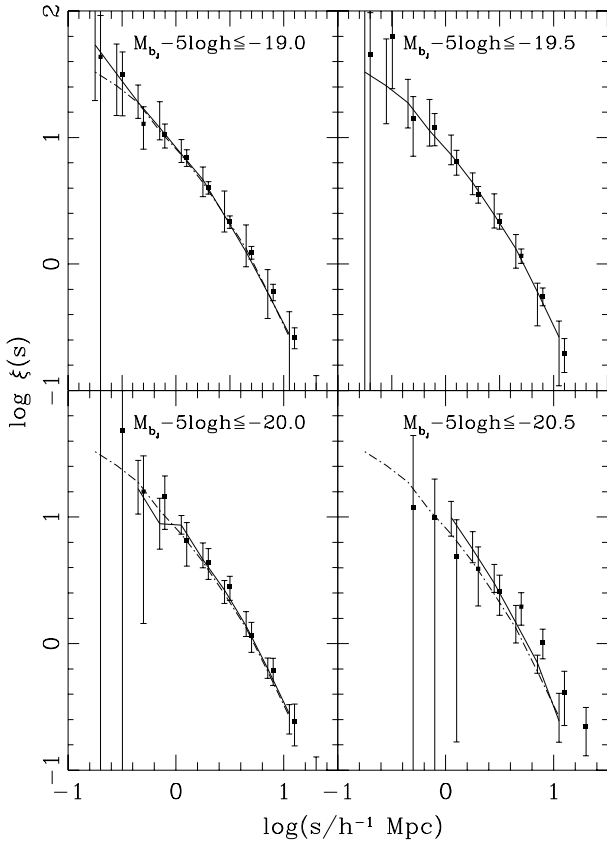


Figure 7. Redshift-space correlation functions of galaxies selected by b_J -band absolute magnitude (see panels for magnitude cuts). The lines show the median model correlation function obtained from fifty randomly chosen volumes equal in size to the corresponding ESP sample. The error bars on these lines indicate the 10% and 90% intervals of the distribution of correlation functions. The model result for $M_{b_J} - 5 \log h \leq -19.5$ is reproduced, for reference, in each panel as the dot-dashed line. The filled squares with error bars show the correlation functions estimated from the volume-limited samples of the ESP (Guzzo et al. 1999).

Guzzo et al. (1999) argue that for the brightest magnitude cut they considered, $M_{b_J} - 5 \log h \leq -20.5$, there is evidence for stronger clustering than for galaxies with $M_{b_J} - 5 \log h \leq -19.5$. Unfortunately, this effect is most noticeable on scales somewhat larger than those we can probe reliably with our simulation. At $r \sim 10h^{-1}\text{Mpc}$, the largest scale on which we can reliably measure the correlation function, we find that galaxies with $M_{b_J} - 5 \log h \leq -20.5$ have a clustering amplitude that is only 1.07 ± 0.10 times greater than that of galaxies with $M_{b_J} - 5 \log h \leq -19.5$ (when measured from the full volume of our simulation). Thus, the results from the GIF simulation are inconclusive. We have therefore made use of the 512^3 simulation, described in §2, to examine the clustering of very bright galaxies. The correlation function of galaxies brighter than $M_{b_J} - 5 \log h = -20.5$ in this simulation agrees with that of the same galaxies in the GIF simulation, within the rather large errorbars (due to the limited number of such bright galaxies in the GIF

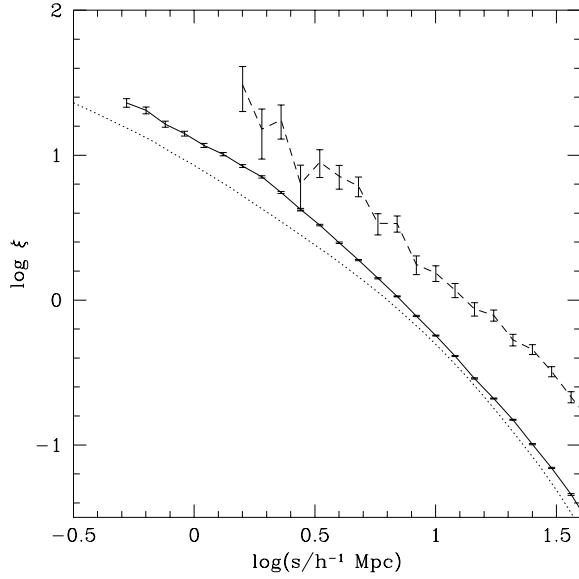


Figure 8. Redshift-space correlation functions of galaxies brighter than $M_{b_J} - 5 \log h = -20.5$ (solid line) and -21.5 (dashed line) measured in the 512^3 simulation. The redshift-space correlation function of dark matter in this simulation is shown by the dotted line.

volume), except on the largest scales where the different dark matter correlation functions in the simulations (as discussed in §2) introduce a similar difference in the galaxy correlation functions. As shown in Fig. 8, we find that, in the 512^3 simulation, galaxies with $M_{b_J} - 5 \log h \leq -21.5$ have a clustering amplitude on scales above $10h^{-1}\text{Mpc}$ which is approximately 4 times higher than that of galaxies with $M_{b_J} - 5 \log h \leq -20.5$. The space densities of $M_{b_J} - 5 \log h \leq -20.5$ and -21.5 galaxies are approximately 6 and 200 times lower than that of L_* galaxies respectively. The large increase in clustering amplitude is due to the fact that these very bright galaxies are found mostly in halos of mass $\gtrsim M_*$, for which the halo bias is a rapidly changing function of halo mass (Mo & White 1996).

In Fig. 9 we show the real-space correlation function for our models applying the same four absolute magnitude cuts. Guzzo et al. (1999) estimated the real-space correlation function by fitting a power-law to the correlation function measured in terms of projected separation. We plot their results over the range of scales used in their fit, $0.5 \leq r \leq 9.5h^{-1}\text{Mpc}$. Within the estimated errors from sample variance, our models are in reasonable agreement with the measurements. Guzzo et al. claim to find evidence for a weak luminosity dependence in the real-space correlation function, with galaxies in the brightest magnitude cut being the most strongly clustered. This effect is manifest as an increase in the correlation length with intrinsic luminosity obtained from their power-law fits to the correlation function. The slope of the ESP correlation function also increases for intrinsically brighter galaxies. In contrast, we find no significant evidence for a luminosity dependence of either clustering length or the slope of the correlation function in our models. The pair-counting errors that Guzzo et al. estimated for the fitted parameters are largest for the

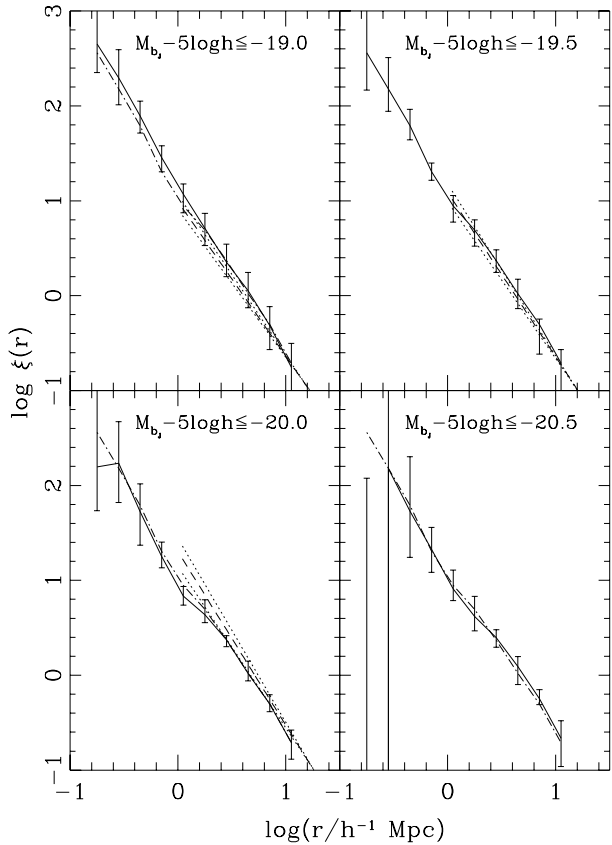


Figure 9. Real-space correlation functions of galaxies selected by b_J -band absolute magnitude (see panels for magnitude cuts). The dashed lines show the power-law fits to the corresponding ESP survey correlation functions obtained by Guzzo et al. (1999). Dotted lines track the quoted errors on these fits. The solid line in each panel shows the median model correlation function obtained by splitting our sample into fifty randomly positioned cubes with volume equal to that of the ESP survey at the same magnitude cut. Error bars on this line indicate the 10% and 90% intervals of the distribution from these same samples. The model result for $M_{b_J} - 5 \log h \leq -19.5$ is reproduced, for reference, in each panel as the dot-dashed line.

brightest sample, which contains the fewest galaxies. Our model correlation functions, however, indicate that sample variance is particularly significant for the *fainter* catalogues, which sample smaller volumes. Taking this sample variance into account weakens the significance of the effect claimed by Guzzo et al.

To confirm that our model predictions for $\xi(r)$ are robust, we follow Benson et al. (2000) and consider the effect on the correlation function of galaxies of varying key parameters in our semi-analytic model, for example, the galaxy merger rate or the baryon fraction. Each model is constrained to match the ESP b_J -band luminosity function at L_* by adjusting the parameter Υ , which gives the ratio of the total mass in stars (including brown dwarfs) to that in luminous stars. (See Benson et al. (2000) for a description of these variant models.)

In Fig. 10 we show the real-space correlation functions

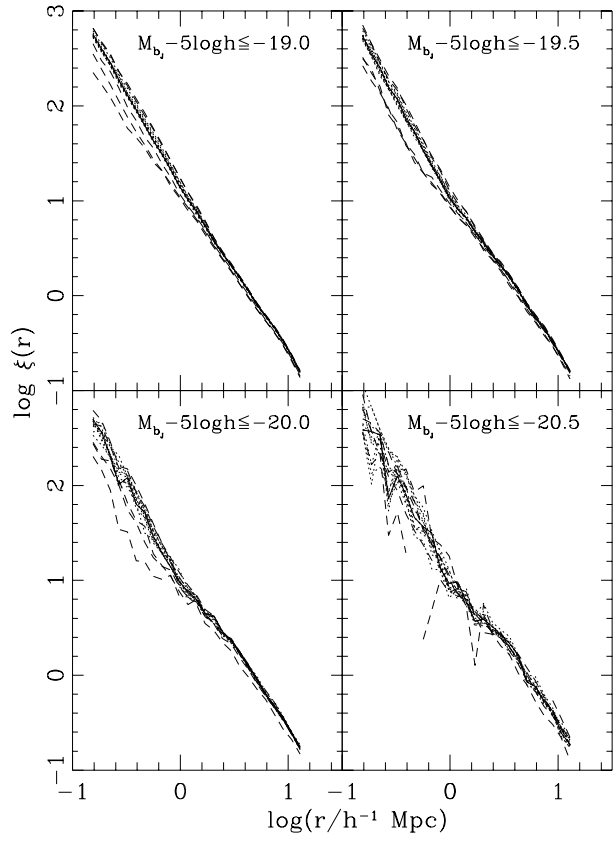


Figure 10. Real-space correlation functions of galaxies selected by b_J -band absolute magnitude (see panels for magnitude cuts). The fifteen variant models are plotted either as dotted lines if they produce a correlation function similar to the standard model or as dashed lines if they do not.

obtained from the fifteen models with altered parameter values. Of the fifteen variants considered, five exhibit significantly different clustering properties to the fiducial model. As can be seen in Fig. 11, these models are amongst the ones that disagree the most with the observed luminosity function, where these models are shown as dashed lines. This highlights again the point emphasized by (Benson et al. 2000) that a good fit to the galaxy luminosity function is a pre-requisite for a robust determination of clustering statistics in semi-analytic models. The same five models were shown as dashed lines in Fig. 6, were they show a greater variation in velocity dispersions than models which are a good fit to the luminosity function. This shows that reproducing the bright end of the luminosity function is also important in order to make robust predictions for galaxy velocity statistics.

4.2 Dependence of clustering on morphology

In Fig. 12, we compare the real-space correlation functions for galaxies selected by morphological type in our model with observational data from Loveday et al. (1995). Although we restrict attention to galaxies in the same magnitude range used by Loveday et al., our criteria for mor-

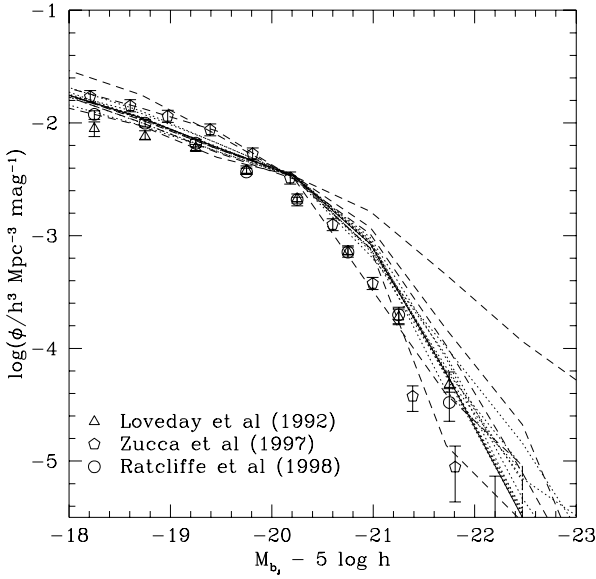


Figure 11. The local b_J -band luminosity function. Symbols with error bars show various observational estimates of this quantity, as indicated in the legend. The lines show fifteen variant models along with our standard model (solid line). The five models which show significantly different correlation functions are identified by dashed lines.

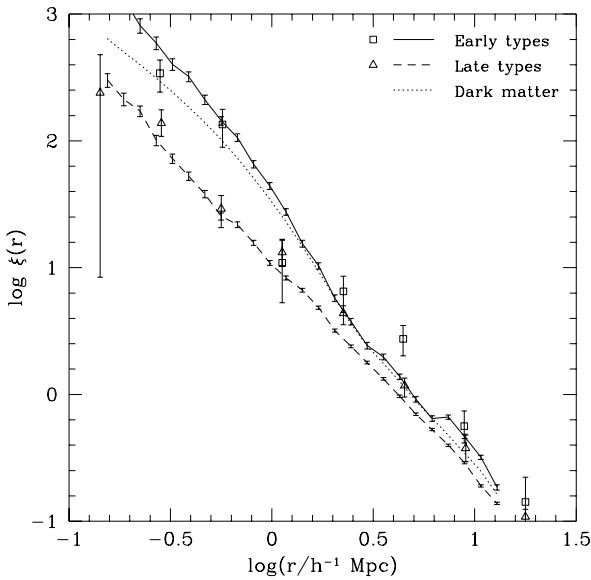


Figure 12. Real-space two-point correlation function for galaxy samples selected by morphological type. Squares and triangles with error bars show the observed correlation functions of early and late type galaxies respectively, with $-20.0 < M_{b_J} - 5 \log h < -19.0$, from Loveday et al. (1995). Solid and dashed lines show correlation functions for model galaxies in the same magnitude range. This sample is subdivided by morphological type as described in the text. For the model, the lines indicate the correlation function from the whole simulation volume, which is approximately 1.3 times larger than the $M_{b_J} - 5 \log h < -19.0$ volume-limited Stromlo-APM survey. The dotted line shows the correlation function of the dark matter.

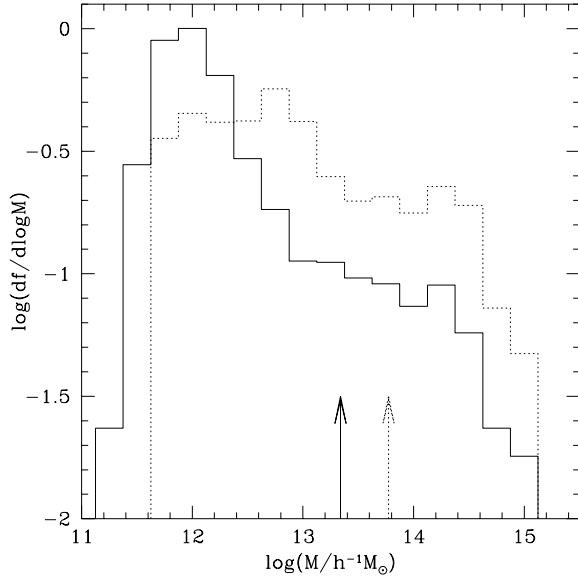


Figure 13. The mass function of host dark matter halos, weighted by the number of galaxies with $-20.0 < M_{b_J} - 5 \log h < -19.0$ per halo, for late type galaxies (solid line) and early type galaxies (dotted line) in our model. The mass functions are normalised by the total number of galaxies in each sample. The arrows indicate the mean host halo mass for each population of galaxies.

phological classification are inevitably somewhat different. Loveday et al. classified galaxies by eye as either early types (E/SO) or late types (S/Irr). Our classification is based on the bulge-to-total luminosity ratio of each galaxy as measured in dust-extincted B-band light (B/T). We classify galaxies with $B/T < 0.4$ as late type galaxies and those with $B/T > 0.4$ as early type galaxies. The observed correlation between bulge-to-total luminosity ratio and morphological type displays a large scatter (see Fig. 1 of Baugh, Cole & Frenk 1996b).

Bearing these caveats in mind, the level of agreement between the observed correlation functions and the model predictions shown in Fig. 12 is encouraging. Early type galaxies are the most strongly clustered on all the scales we consider, as found also by Kauffmann et al. (1999a). The greatest difference occurs on scales below $1h^{-1}$ Mpc, where early type galaxies have a clustering amplitude that is more than 4 times higher than that of late type galaxies. On larger scales, the difference in clustering amplitudes persist, but is less pronounced.

In Fig. 13, we plot the host halo mass functions of late and early type galaxies in our model (weighted by the number of galaxies per halo). As may be seen, early type galaxies do, on average, reside preferentially in higher mass environments than late type galaxies, as speculated by Loveday et al. (1995). This explains the larger correlation length of the early types since higher mass halos are intrinsically more strongly biased (Frenk et al. 1988, Mo & White 1996) relative to the dark matter distribution as a whole. It also explains the greater correlation amplitude of early type galaxies on scales below $1h^{-1}$ Mpc, where the correlation function is sensitive to the number of galaxy pairs inside cluster sized

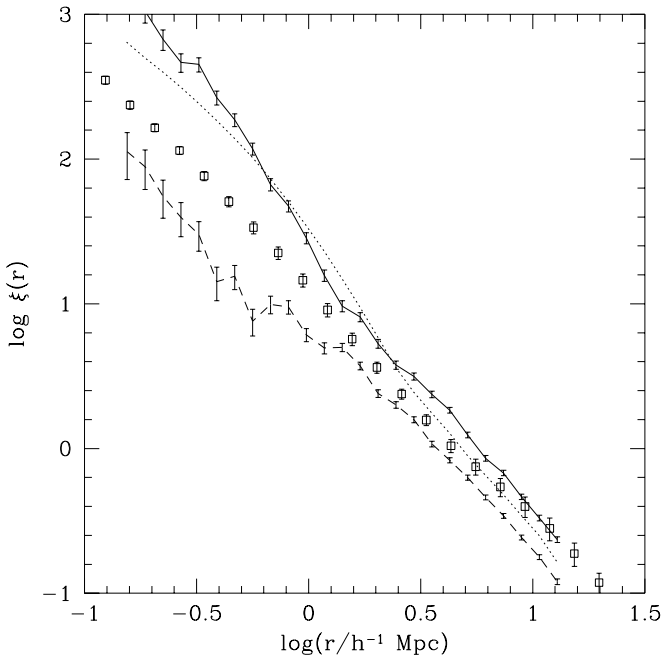


Figure 14. The real-space correlation function of galaxies brighter than $M_B - 5 \log h = -19.5$ in our model selected by B-R colour. The solid line is the correlation function of galaxies with $B-R > 1.3$, whilst the dashed line is that of galaxies with $B-R \leq 1.3$. Error bars on these lines show the Poisson pair counting errors. The dotted line shows the correlation function of the dark matter, and the points with error bars are the real-space correlation function measured from the APM survey for all galaxies (Baugh 1996).

halos (Benson et al. 2000). Late type galaxies are rare in these halos and so their pair count on these scales is small, resulting in a lower correlation amplitude.

4.3 Dependence of clustering on colour

At present, the only available observational constraints on the colour dependence of galaxy clustering come from deep, magnitude-limited samples that cover a significant baseline in redshift. The technique used in this paper needs to be extended to include evolution both in the galaxy population and in the clustering of dark matter to produce realistic mock catalogues that can be compared with these observations. We defer a detailed discussion of these techniques and a thorough comparison to the data to a later paper (Benson et al. 2000). However, forthcoming redshift surveys, such as the 2dF (Colless 1996) and SDSS (Gunn & Weinberg 1995), will contain large enough numbers of galaxies with photometry in different bands to allow the construction of local volume-limited samples subdivided by galaxy colour.

We present, in Fig. 14, our predictions for colour dependent clustering of galaxies in real space, measured in the full volume of our simulation. Red galaxies are defined to have $B-R > 1.3$ and blue galaxies $B-R \leq 1.3$, which matches the cut used by Willmer, da Costa & Pellegrini (1998). The error bars show the Poisson pair counting errors in each bin. The clustering of red galaxies is significantly stronger than that of blue galaxies, which follows from the fact that the

red galaxies are predominantly early types, and so are predicted to reside preferentially within higher mass halos than the blue galaxies.

5 DISCUSSION

In this paper, we have combined N-body simulations of the hierarchical clustering of dark matter with semi-analytic modelling of the physics of galaxy formation, to probe the relationship between the distribution of galaxies and the distribution of mass in a Λ -dominated cold dark matter universe.

In an earlier paper (Benson et al. 2000), we studied the correlation function of galaxies brighter than L_* in *real-space* (i.e. as a function of true spatial separation; see also Kauffmann et al. 1999a). We found remarkably good agreement between the predictions of the Λ CDM model and measurements of the correlation function of the APM galaxy survey (Baugh 1996), over four orders of magnitude in correlation amplitude. On small scales, we found the model galaxies to be *less strongly* clustered than (or biased low relative to) the dark matter. We have now seen that the net effect of small-scale peculiar velocities is to cancel out this bias: in redshift space the galaxy and dark matter correlation functions are very similar to one another. This cancellation arises because the pairwise velocity dispersions of galaxies and dark matter are different. Fortunately, the difference is just sufficient to compensate for the differences in real-space clustering. Thus, although genuinely biased, the distribution of galaxies measured in redshift space appears, to a good approximation, unbiased on small scales. The pairwise velocity dispersion of the model galaxies is $\sim (200 - 300)$ km/s lower than that of the dark matter over almost two decades in spatial separation and is in good agreement with recent observational determinations (Jing, Mo & Börner 1998). However, comparison of our results with those of Kauffmann et al. (1999a) demonstrates the sensitivity of this statistic to the number of galaxies that populate rich clusters. Both models are consistent with the available data for the Coma cluster, but produce line-of-sight velocity dispersions which differ by around 100 km/s.

The physical origin of the offset between the galaxy and dark matter velocity distributions lies in the way in which galaxies sample the velocity field of the dark matter. The mass-to-light ratio of halos in our model is a strong, non-monotonic function of halo mass. Galaxy formation is most efficient in halos of mass $\sim 10^{12} h^{-1} M_\odot$, and the mass-to-light ratio increases at higher and lower masses due to long cooling times for the gas and stronger feedback respectively (see Fig. 8 of Benson et al. 2000). As a result, the number of galaxies per halo does not increase as rapidly as the halo mass. Thus, when computing the pairwise velocity dispersion, high velocity dispersion halos are undersampled by galaxies relative to the contribution of these halos to the velocity dispersion of the dark matter itself.

We have explored the sensitivity of our theoretical predictions for peculiar velocities to variations in the galaxy formation parameters. In Benson et al. (2000) we found that predictions for the galaxy two-point correlation function in a particular cosmological model are robust to changes in model parameters, provided that the galaxy luminosity func-

tion remains approximately the same. Here, we find a similar result for the peculiar velocities: models with similar luminosity functions produce similar results. The amplitude of the velocity bias depends not only on the luminosity function, but also on the shape of the power spectrum of density fluctuations and on the statistics of the occupation of halos by galaxies. As we showed in Benson et al. (2000), our (cluster-normalized) Λ CDM model gives a good match to the observed luminosity function of galactic systems. To a large extent, this is the reason why the model also gives a good match to the observed pairwise velocity dispersion function (although our neglect of dynamical biases in the galaxy distribution may affect our results slightly). The differences between our predicted peculiar velocities and those obtained by Kauffmann et al. (1999a) from the same N-body simulations, but using a different semi-analytic model, are simply due to differences in the way in which the two models populate high mass halos. These, in turn, reflect differences in the luminosity functions of galaxies and galactic systems in the two models.

The dependence of clustering on intrinsic galaxy properties provides, in principle, an interesting test of models of galaxy formation. The most obvious property to consider is galaxy luminosity. Unfortunately, the dependence of clustering on luminosity is difficult to measure from magnitude limited redshift surveys and so the observational situation is inconclusive. A weak effect has been claimed, for example, by Guzzo et al. (1999) for galaxies approximately one magnitude brighter than L_* . For the bulk of the galaxy population, we find no evidence for a dependence of clustering on the intrinsic luminosity of our model galaxies. This is not surprising in view of the fact that galaxies of a given luminosity reside in dark matter halos spanning an appreciable range of masses. We do, however, predict a strong effect for galaxies that are significantly brighter than L_* . Unfortunately, the space density of these galaxies is too low for their clustering to be measured in existing redshift surveys. On the other hand, both models and observations agree that early type or red galaxies are more strongly clustered than late type or blue galaxies, particularly on small scales. This is a reflection of the observed morphology-density relation which arises naturally in hierarchical clustering models (Frenk et al. 1985, Kauffmann 1996, Baugh, Cole & Frenk 1996b).

It is worth emphasizing that the galaxy formation model that we have used in this paper is essentially the same as that discussed at length in Cole et al. (1999) (except for the small differences mentioned in §2) and adopted by Benson et al. (2000). Cole et al. fixed parameter values by requiring their model to reproduce a variety of properties of the local galaxy population, with emphasis placed on achieving a good match to the local b_J -band galaxy luminosity function. This same Λ CDM model also reproduces the present day clustering of galaxies in real and redshift space, is in reasonable agreement with the observed line-of-sight pairwise velocity dispersion of galaxies, and matches the clustering measured at intermediate and high redshifts (Baugh et al. 1999).

An important conclusion of this work is that the statistical properties of the galaxy distribution can be quite different from those of the underlying dark matter. A physical approach to modelling the formation and evolution of galaxies, using the kind of techniques discussed in this pa-

per and also in Kauffmann et al. (1999a) and Benson et al. (2000), is therefore imperative if we are to understand the biases in the way that different galaxies trace the dark matter. This, in turn, is a pre-requisite for making sense of the unprecedented amount of information about the galaxy distribution in the low and high redshift Universe that will shortly become available from forthcoming redshift surveys.

ACKNOWLEDGEMENTS

AJB, SMC, CSF and CGL acknowledge receipt of a PPARC Studentship, Advanced Fellowship, Senior Fellowship and Visiting Fellowship respectively. CSF further acknowledges receipt of a Leverhulme Fellowship. This work was supported in part by a PPARC rolling grant, by a computer equipment grant from Durham University and by the European Community's TMR Network for Galaxy Formation and Evolution. We acknowledge the Virgo Consortium and the GIF collaboration for making available the GIF simulations for this study and the VIRGO Consortium for providing the other N-body simulations used in this work. We thank Simon White and Nigel Metcalfe for many valuable comments, and the referee Antonaldo Diaferio both for supplying his galaxy catalogue and for providing critical and useful comments which improved the clarity of this paper.

REFERENCES

Alimi J.-M., Valls-Gabaud D., Blanchard A., 1988, A&A, 206, L11
Bardeen J. M., Bond J. R., Kaiser N., Szalay A. S. 1986, ApJ, 304, 15
Baugh C. M., 1996, MNRAS, 280, 267
Baugh C. M., Cole S., Frenk C. S., 1996a, MNRAS, 282, L27
Baugh C. M., Cole S., Frenk C. S., 1996b, MNRAS, 283, 1361
Baugh C. M., Cole S., Frenk C. S., Lacey C. G., 1998, ApJ, 498, 504
Baugh C. M., Benson A. J., Cole S., Frenk C. S., Lacey C. G., 1999, MNRAS, 305, L21
Benoist C., Maurogordato S., da Costa L. N., Cappi A., Schaeffer R., 1996, ApJ, 472, 452
Benson A. J., Cole S., Frenk C. S., Baugh C. M., Lacey C. G., 2000, MNRAS, 311, 793
Benson A. J., Cole S., Frenk C. S., Baugh C. M., Lacey C. G., 2000, in preparation
Bond J. R., Efstathiou G., 1984, ApJ, 285, L45
Bond J. R., Kaiser N., Cole S., Efstathiou G., 1991, ApJ, 379, 440
Bower R. G., 1991, MNRAS, 248, 332
Carlberg R. G., Cowie L. L., Songaila A., Hu E. M., 1997, ApJ, 484, 538
Cole S., Aragón-Salamanca A., Frenk C. S., Navarro J. F., Zepf S. E., 1994, MNRAS, 271, 781
Cole S., Lacey C. G., Baugh C. M., Frenk C. S., 1999, submitted to MNRAS
Colín P., Klypin A., Kravtsov A., Khokhlov A., 1999, ApJ, 523, 32
Colless M., 1996, in proceedings of the Heron Island Conference, <http://msowww.anu.edu.au/~heron/Colless/colless.html>
Davis M., Geller M. J., 1976, ApJ, 208, 13
Davis M., Peebles P. J. E., 1983, ApJ, 267, 465
Davis M., Efstathiou G., Frenk C. S., White S. D. M., 1985, ApJ, 292, 371
Davis M., Meiskin A., Strauss M. A., da Costa L. N., Yahil A., 1988, ApJ, 333, L9
Diaferio A., Kauffmann G., Colberg J. M., White S. D. M., 1999, MNRAS, 307, 537

Dressler A., 1980, *ApJ*, 236, 351

Eke V. R., Cole S., Frenk C. S., 1996, *MNRAS*, 282, 263

Ferrara A., Bianchi S., Cimatti A., Giovanardi C., 1999, *ApJS*, 123, 437

Frenk C. S., White S. D. M., Davis M., Efstathiou G., 1988, *ApJ*, 327, 507.

Frenk C. S., White S. D. M., Efstathiou G., Davis M., 1985, *Nat*, 327, 595.

Geller M. J., Diaferio A., Kurtz M. J., 1999, *ApJ*, 517, L23

Giovanelli R., Haynes M. P., Chincarini G. L., 1986, *ApJ*, 300, 77

Godwin J. G., Metcalfe N., Peach J. V., 1983, *MNRAS*, 202, 113

Governato F., Baugh C. M., Frenk C. S., Cole S., Lacey C. G., Quinn T., Stadel J., 1998, *Nat*, 392, 359

Gunn J. E., Weinberg D. H., 1995, *Wide-Field Spectroscopy and the Distant Universe*, proceedings of the 35th Herstmonceux workshop, Cambridge University Press, Cambridge

Guzzo L. et al., 1999, submitted to *A&A* astro-ph/9901378

Hamilton A. J. S., 1988, *ApJ*, 331, L59

Hamilton A. J. S., 1992, *ApJ*, 385, 5

Hoyle F., Baugh C. M., Shanks T., Ratcliffe A., 1999, *MNRAS*, 309, 659

Infante L., Pritchett C. J., 1993, *ApJ*, 439, 565

Iovino A., Giovanelli R., Haynes M., Chincarini G., Guzzo L., 1993, *MNRAS*, 265, 21

Jenkins A., Frenk C. S., Pearce F. R., Thomas P. A., Colberg J. M., White S. D. M., Couchman H. M. P., Peacock J. A., Efstathiou G., Nelson A. H., (the VIRGO Consortium), 1998, *ApJ*, 499, 20

Jing Y. P., Mo H. J., Börner G., 1998, *ApJ*, 494, L1.

Kaiser N., 1984, *ApJ*, 284, L9

Kaiser N., 1987, *MNRAS*, 227, 1

Kauffmann G., White S. D. M., Guiderdoni B., 1993, *MNRAS*, 264, 201

Kauffmann G., Guiderdoni B., White S. D. M., 1994, *MNRAS*, 267, 981

Kauffmann G., 1996, *MNRAS*, 281, 487

Kauffmann G., Charlot S., White S. D. M., 1996, *MNRAS*, 283, 117

Kauffmann G., Nusser A., Steinmetz M., 1997, *MNRAS*, 286, 795

Kauffmann G., Colberg J. M., Diaferio A., White S. D. M., 1999a, *MNRAS*, 303, 188

Kauffmann G., Colberg J. M., Diaferio A., White S. D. M., 1999b, *MNRAS*, 307, 529

Kolatt T. S., Bullock J. S., Somerville R. S., Sigad Y., Jonsson P., Klypin A. A., Primack J. R., Faber S. M., Dekel A., 1999, *ApJ*, 523, L109

Lacey C. G., Guiderdoni B., Rocca-Volmerange B., Silk J., 1993, *ApJ*, 402, 15.

Lacey C. G., Cole S., 1993, *MNRAS*, 262, 627

Lacey C. G., Cole S., 1994, *MNRAS*, 271, 676

Lahav O., Rees M. J., Lilje P. B., Primack J. R., 1991, *MNRAS*, 251, 128

Landy S. D., Szalay A. S., Koo D. C., 1996, *ApJ*, 460, 94

Le Fèvre O., Hudon D., Lilly S. J., Crampton D., Hammer F., Tresse L., 1996, *ApJ*, 461, 534

Lemon G., Kauffmann G., 1999, *MNRAS*, 302, 111

Loveday J., Peterson B. A., Efstathiou G., Maddox S. J., 1992, *ApJ*, 390, 338

Loveday J., Maddox S. J., Efstathiou G., Peterson B. A., 1995, *ApJ*, 442, 457

Marzke R. O., Geller M. J., da Costa L. N., Huchra J. P., 1995, *AJ*, 110, 477

Mo H. J., Jing Y. P., Börner G., 1993, *MNRAS*, 264, 825

Mo H. J., Jing Y. P., Börner G., 1997, *MNRAS*, 286, 979

Mo H. J., White S. D. M., 1996, *MNRAS*, 282, 347

Moore B., Frenk C. S., White S. D. M., 1993, *MNRAS*, 261, 827

Moore B., Frenk C. S., Efstathiou G., Saunders W., 1994, *MNRAS*, 269, 742

Park C., Vogeley M. S., Geller M. J., Huchra J. P., 1994, *ApJ*, 431, 569

Pearce F. R., Jenkins A., Frenk C. S., Colberg J. M., White S. D. M., Thomas P. A., Couchman H. M. P., Peacock J. A., Efstathiou G. (The VIRGO Consortium), 1999, *ApJ*, 521, 99

Peebles P. J. E., 1980, *The Large-Scale Structure of the Universe*, Princeton

Press W. H., Schechter P., 1974, *ApJ*, 187, 425

Phillipps S., Shanks T., 1987, *MNRAS*, 229, 621

Ratcliffe A., Shanks T., Parker Q. A., Fong R., 1998a, *MNRAS*, 293, 197

Ratcliffe A., Shanks T., Parker Q. A., Fong R., 1998b, *MNRAS*, 296, 191

Santiago B. X., da Costa L. N., 1990, *ApJ*, 362, 386

Seljak U., Zaldarriaga M., 1996, *ApJ*, 469, 437

Shectman S. A., Landy S. D., Oemler A., Tucker D. L., Lin H., Kirshner R. P., Schechter P. L., 1996, *ApJ*, 470, 172

Somerville R. S., Davis M., Primack J. R., 1997, *ApJ*, 479, 616

Somerville R. S., Primack J. R., Nolthenius R., 1997, *ApJ*, 479, 606

Somerville R. S., Primack J. R., 1999, *MNRAS*, 310, 1087

Somerville R. S., Lemson G., Kolatt T. S., Dekel A., 1998, astro-ph/9807277 (submitted to *MNRAS*)

Tadros H., Efstathiou G., 1996, *MNRAS*, 282, 1381

White, S. D. M., Efstathiou, G., Frenk, C. S., 1993a, *MNRAS*, 262, 1023

White S. D. M., Navarro J. F., Evrard A. E., Frenk C. S., 1993, *Nat*, 366, 429

White S. D. M. & Frenk, C. S., 1991, *ApJ*, 379, 52

White S. D. M., Tully R. B., Davis M., 1988, *ApJ*, 333, 45

Willmer C. N. A., da Costa L. N., Pellegrini P. S., 1998, *AJ*, 115, 869

Zucca E., et al., 1997, *A&A*, 326, 477

Zurek W., Quinn P. J., Salmon T. K., Warren M. S., 1994, *ApJ*, 431, 559